Flow-Induced On-Line Crystallization of Rodlike Molecules in Fiber Spinning

ALEXANDER L. YARIN

Faculty of Mechanical Engineering, Technion, Haifa 32000, Israel

SYNOPSIS

The micromechanical description of nonisothermal flow-induced crystallization of a polymeric liquid with rodlike molecules is the main part of the fiber spinning model described here. Solutions of the governing equations show that an increase in winding velocity leads to the appearance of an on-line flow-induced crystallization zone in a fiber. This zone manifests itself in accelerated formation (necking) due to the release of heat of crystallization which results in the decrease of viscosity. Liquid crystallinity grows very rapidly in the necking region, which, in turn, leads to the growth of viscosity after some minimal value, which finally arrests fiber deformation.

INTRODUCTION

During the last decade, studies connected with advanced fiber spinning technologies have concentrated attention on high-speed fiber spinning with winding velocities of the order of several thousand meters per minute.[1] Under such conditions an elongational flow triggers off a flow-induced orientation and crystallization, which, in its turn, can affect flow in a liquid spinline. Crystallization kinetics description should be incorporated into existing hydrodynamic models of fiber spinning to allow us a theoretical treatment of high-speed processing. Some phenomenological models of nonisothermal flow-induced crystallization have been proposed[1-3] as well as micromechanical models for flexible macromolecules.[1,4]

The objective of the present work is micromechanical description of nonisothermal flow-induced crystallization of rodlike molecules and incorporation of resulting crystallization kinetics into hydrodynamic model of fiber spinning. We take into account the variation of entropy of a liquid due to reorientation of rodlike molecules in an elongational flow inside a fiber. Such reorientation results in a decrease of liquid entropy and increase of the temperature of phase transition liquid/crystal. As a result, an overcooling of liquid particles increases due to stretching and flow-induced crystallization may start in a spinline. Such crystallization leads to a heat release, which, in turn, leads first of all to increased temperature, decrease of viscosity and subsequent rapid diameter attenuation (necking). In the region of accelerated formation part of the liquid rapidly increases in crystallinity leading to the growth of viscosity, which finally completely arrests spinline deformation.

THEORETICAL MODEL

Consider the governing equations for high-speed fiber spinning (see Fig. 1). To describe a flow of a liquid in the fiber spinning, we shall use the quasi-one-dimensional approximation.[1,2,5] Let us consider here a steady flow only. In this case the equations of continuity and momentum for a liquid in a fiber have the form

$$V\pi a^2 = V_0\pi a_0^2 = Q$$

$$\rho Q\frac{dV}{dz} = \frac{d}{dz}\left(3\mu\frac{dV}{dz}\pi a^2\right) - \pi a\rho_1 V^2 0.65\left(\frac{2Va}{\nu_1}\right)^{-0.81} \quad (1)$$

Here the last term on the right-hand side of the

Journal of Applied Polymer Science, Vol. 46, 873-878 (1992)

CCC 0021-8995/92/050873-06

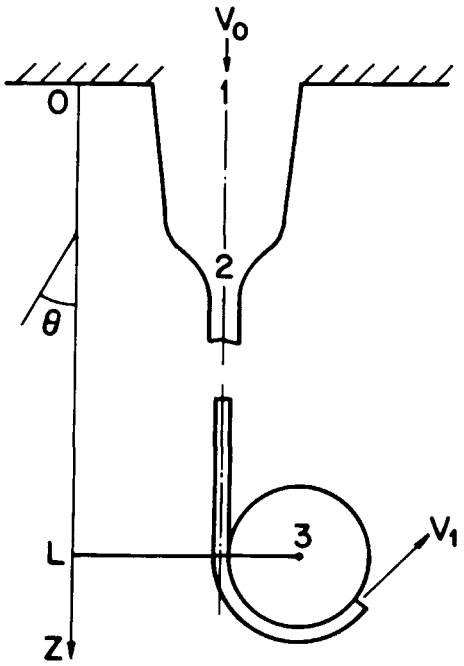

Figure 1 Scheme of high-speed fiber spinning: (1) spinneret hole; (2) necking region in a fiber; (3) winding device.

second equation describes the air friction at the surface of a fiber;[1] V is the longitudinal velocity, a is the cross-section radius, ρ is the density of a liquid, z is the longitudinal coordinate, Q is the volumetric flow rate, ρ_1 and ν_1 are density and kinematic viscosity of air; subscripts 0 here and hereafter mark the known values of parameters at a spinneret hole exit.

Viscosity μ depends both on temperature T and degree of crystallinity η_c (the part of material which was crystallized):

$$\mu = \mu^* \exp\left(\frac{E}{RT}\right) \exp(B\eta_c^b) \qquad (2)$$

Here μ^* is preexponential factor, E is activation energy, R is gas constant, and B and b are nondimensional constants (material constants).

We introduce c as a concentration of nuclei of crystallization which may grow (the units of c are $1/m^3$). We consider a growth of fibrillar cylinderlike crystals with a diameter of a cross-section d and rate of linear growth v. In unit time in a unit volume of liquid appears crystalline volume $2(\pi d^2/4)vc(1 - \eta_c)$. Thus, the thermal balance equation in a fiber has the form

$$\rho c_1 Q \frac{dT}{dz} = -\pi(T - T_\infty)\Lambda_1 0.42\left(\frac{2Va}{\nu_1}\right)^{0.334} + \rho\pi a^2 \Delta h^0 (1 - \eta_c)\frac{\pi d^2}{2} vc + 3\mu\left(\frac{dV}{dz}\right)^2 \pi a^2 \qquad (3)$$

Here c_1 is a specific heat of a liquid, T_∞ is air temperature at the infinity, Λ_1 is thermal conductivity of air, and Δh^0 is heat release of crystallization of a unit mass.

The empirical law for the convective heat transfer at fiber surface incorporated into (3) (the first term on the right-hand side) is widely used in studies of fiber spinning.[1] The second term on the right-hand side of (3) describes heat release in a crystallization process (we neglect here the difference between densities of liquid and crystalline phases), and the third one describes the dissipation of energy. As usual, we neglect the conductive heat transfer along a fiber.

The equations describing the appearance of nuclei which may grow, and the increase of crystalline phase are as follows:

$$\frac{dc}{dt} = I(t), \quad \frac{d\eta_c}{dt} = (1 - \eta_c)\frac{\pi d^2}{2} vc \qquad (4)$$

Here $I(t)$ is a rate of nucleation in a unit volume (we take into account only the nuclei which are large enough to start to grow); the units of I are $1/(m^3 s)$; d/dt denotes material time differentiation ($d/dt = Vd/dz$). In Ref. 6 the term "rate equations" was proposed for equations of such a type.

Equations (1)–(4) should be solved with the boundary conditions as follows:

$$z = 0, \quad V = V_0, \quad T = T_0, c = 0, \quad \eta_c = 0$$
$$z = L, \quad V = V_1 \qquad (5)$$

Equations (4) may be rearranged to the integral form

$$\eta_c = 1 - \exp\left\{\frac{\pi d^2}{2}\int_0^{vt}\left[\int_0^{t - r/v} I(\tau)\, d\tau\right]dr\right\} \qquad (6)$$

which is the generalization of Avrami's law for nonisothermal flow-induced crystallization.

RATE OF NUCLEATION

We calculate the rate of nucleation, I, incorporated into the system of governing equations (1)–(4).

From the thermodynamics of polymers,[7,8] we have the formulae for the melt temperature T_m and specific free enthalpy (Gibbs potential) change $\Delta\varphi$ in a slow equilibrium crystallization process:

$$T_m = \frac{T_m^0}{1 + (S_1 - S_1^0)T_m^0/(M\Delta h^0)}$$

$$\Delta\varphi = \Delta h^0 \rho_{pc}\left(1 - \frac{T}{T_m}\right) \tag{7}$$

Here S_1 is entropy of a liquid phase, M is molecular mass of a monomer, ρ_{pc} is density of a crystalline polymer; superscripts 0 mark the values of parameters corresponding to the crystallization of an unoriented isotropic liquid.

The orientation probability density function W for a rodlike molecule in uniaxial elongational flow inside of a fiber is described by the equation as follows:

$$\frac{\partial W}{\partial t} = \frac{3}{4}\dot{\gamma}\sin 2\theta \frac{\partial W}{\partial \theta} + \frac{3}{2}\dot{\gamma}W(2\cos^2\theta - \sin^2\theta) \tag{8}$$

In eq. (8) $\dot{\gamma} = dV/dz$ is rate of strain along the fiber axis $0z$; θ is an angle in spherical coordinate system between radius–vector and $0z$–axis ($0 \leq \theta \leq \pi$, see Fig. 1).

Equation (8) is a particular case of the Fokker–Planck equation. We have neglected rotational Brownian diffusion of rodlike molecules, which is justified if the rotational diffusion constant $D_r \ll \dot{\gamma}$. Using the data of Refs. 9 and 10, we estimate the value of D_r in semidilute solutions as $D_r \sim 1$ s^{-1}; in liquid crystalline phase D_r is smaller. A typical value of $\dot{\gamma}$ corresponding to high-speed fiber spinning is $\dot{\gamma} \sim 10$ s^{-1} (an order of magnitude larger than the above-mentioned value of D_r), which justifies the omission of rotational Brownian diffusion in (8).

In the case of an isotropic initial state of a liquid, when $W = 1/(4\pi)$ at $t = 0$ ($z = 0$) the solution of eq. (8) is as follows:

$$W = \frac{\Lambda^3}{4\pi(\cos^2\theta + \Lambda^3\sin^2\theta)^{3/2}} \tag{9}$$

Here

$$\Lambda = \exp\left[\int_0^t \dot{\gamma}(t')dt'\right] = \frac{V}{V_0} \tag{10}$$

The molar entropy of a liquid according to Boltzmann principle with the account of (9) equals

$$S_1 = R\ln W = R\ln\frac{\Lambda^3}{4\pi(\cos^2\theta + \Lambda^3\sin^2\theta)^{3/2}} \tag{11}$$

For an unoriented liquid we have respectively

$$S_1^0 = R\ln\frac{1}{4\pi} \tag{12}$$

Combining (7), (11), and (12), we obtain the melt temperature of a fibrillar crystal growing at an angle θ to a fiber axis:

$$T_m = \frac{T_m^0}{1 + T_m^0 R\ln[\Lambda^3(\cos^2\theta + \Lambda^3\sin^2\theta)^{-3/2}]/(M\Delta h^0)} \tag{13}$$

Expression (13) corresponds only to equilibrium (or close to equilibrium) rather slow processes of crystallization. It should be used only at extremely low degrees of liquid particle elongation $\Lambda \to 1 + 0$. However, it is known that, at high degrees of orientation, the crystallization process is a "burst"-like one (in high-speed fiber spinning the values of Λ may be of the order of 10^2). In the whole range of variation of Λ, the following equation may be used:

$$T_m = T_m^0\left[\frac{\Lambda^3}{(\cos^2\theta + \Lambda^3\sin^2\theta)^{3/2}}\right]^{-n}, \qquad n = \frac{T_m^0 R}{M\Delta h^0} \tag{14}$$

Equation (13) is the asymptote of (14) as $\Lambda \to 1 + 0$.

We consider a nucleus of fibrillar crystal in the form of a circular cylinder of length l and cross-section area A. The change of the free enthalpy (Gibbs potential) of a system liquid/crystal due to the appearance of a fibrillar nucleus equals

$$\Delta\Phi = 2l(\pi A)^{1/2}\sigma_t + 2A\sigma_e - lA\Delta\varphi \tag{15}$$

where σ_t and σ_e are lateral and edge surface energies.

The minimal sizes of nuclei which may grow correspond to the maximum of $\Delta\Phi$.[7,8] Hence, using (15) and the second expression of (7), the threshold value of $\Delta\Phi$ equals

$$\Delta\Phi_*(\theta) = \frac{8\pi\sigma_t^2\sigma_e}{(\Delta h^0\rho_{pc})^2[1 - T/T_m(\theta)]^2} \tag{16}$$

The probability of appearance of a nucleus (which may grow) oriented at some angle θ equals

$$p = \begin{cases} \exp\left[-\dfrac{\Delta\Phi_*(\theta)}{kT}\right], & T < T_m(\theta) \\ 0, & T > T_m(\theta) \end{cases} \quad (17)$$

where k is the Boltzmann constant.

Hence, the nucleation rate in a unit volume equals

$$I = \frac{Kc_1}{2}\frac{kT}{h}\exp\left(-\frac{E}{RT}\right)\int_0^\pi f(\theta)\,d\theta$$

$$f(\theta) = \begin{cases} \dfrac{\Lambda^3 \sin\theta}{(\cos^2\theta + \Lambda^3\sin^2\theta)^{3/2}} \\ 0, \quad T > T_m(\theta) \end{cases}$$

$$\times \exp\left\{-\frac{U}{RT[1 - T/T_m(\theta)]^2}\right\}, \quad T < T_m(\theta)$$

$$U = \frac{8\pi\sigma_t^2\sigma_e N_A}{(\Delta h^0 \rho_{pc})^2} \quad (18)$$

[eqs. (9), (16) and (17) have been used]. Here K is the reciprocal mean number of molecules per nucleus, c_1 is concentration of molecules, h is Planck's constant, and N_A is Avogadro's number.

Suppose that the value of $U/(RT_0)$ is large enough (which is frequently a case in applications) and evaluate the integral in (18) by using the Laplace asymptotic method.[11] As a result, we obtain

$$I = \frac{Kc_1}{2}\frac{kT}{h}\exp\left(-\frac{E}{RT}\right)$$

$$\times \exp\left\{-\frac{U}{RT[1 - T/(T_m^0\Lambda^N)]^2}\right\}$$

$$\times \left(\frac{2\pi RT_0}{UD}\right)^{1/2}\Lambda^{-3/2}$$

$$D = \frac{6n(\Lambda^3 - 1)}{[1 - T/(T_m^0\Lambda^N)]^3 T_m^0 \Lambda^{N+3}}, \quad N = \frac{3}{2}n \quad (19)$$

The first expression of (19) shows that the effective melt temperature, which varies (increases) along the fiber, equals:

$$T_{m,\text{eff}} = T_m^0\Lambda^N \quad (20)$$

When $T > T_{m,\text{eff}}$, the rate of nucleation $I = 0$.

Note that in the case of crystallization of a liquid with equilibrium inner structure (when $\Lambda = 1$) the function $I(T)$ described by (19) has a maximum $I_{\max}^0$ at a certain value of T. Equations (19) and (10) give us the closure expressions for the governing equations (1)–(4).

RESULTS AND DISCUSSION

Let us use the following model set of parameters corresponding to high-speed fiber spinning[1,2,10]: $\sigma_t = 10^{-2}$ J/m^2, $\sigma_e = 0.19$ J/m^2, $\rho_{pc} = 1455$ kg/m^3, $\Delta h^0 = 141.8 \cdot 10^4$ J/kg, $T_0 = 568$ K, $E = 44.1$ kJ/mol for $T > 343$ K and $E = \infty$ for $T < 343$ K, $L = 1$ m, $a_0 = 1.5 \times 10^{-4}$ m, $V_0 = 28.404$ m/min, $\rho_1 = 0.946$ kg/m^3, $\nu_1 = 0.23 \times 10^{-4}$ m^2/s, $\rho = 1270$ kg/m^3, $\mu^* = 0.073$ kg/(m s), $c_1 = 1.9 \times 10^3$ J/(kg deg), $\Lambda_1 = 0.0315$ J/(m s deg), $T_\infty = 293$ K, $T_m^0 = 553$ K, $B = 10$, and $b = 5$. The value of the nondimensional parameter $K_* = \pi d^2 v I_{\max}^0 L^2/(2V_0^2)$ used in numerical simulations equals 2×10^4. This order of magnitude of K_* corresponds to the appearance of necking. In the most simulation runs the value of nondimensional power N in the nucleation law (19) equals 0.1.

By using the above values of parameters the system of governing equations has been solved numerically. In the results which follow the nondimensional values have been introduced using the scales: a_0 for a; V_0 for V; L for z; T_0 for T and $T_{m,\text{eff}}$; $I_{\max}^0 \times L/V_0$ for c; $I_{\max}^0$ for I.

In Figures 2 and 3 in the nondimensional form the distributions of V, T, η_c, I, $T_{m,\text{eff}}$ and $T/T_{m,\text{eff}}$ along the fiber axis are shown. In Figure 2 the value of 50 for V corresponds to 1420.2 m/min. In Figure 3 the unity at the vertical axis corresponds to 568 K for T and $T_{m,\text{eff}}$. The unity at $0z$ axes corresponds to $1m$. If fibrillar crystal parameters (cross section diameter d and rate of linear growth v) are known

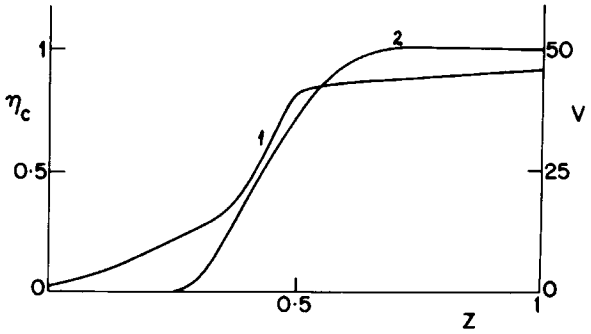

Figure 2 Velocity and crystallinity along a spinline: (1) V; (2) η_c. The value of nondimensional power N in (19) equals 0.1.

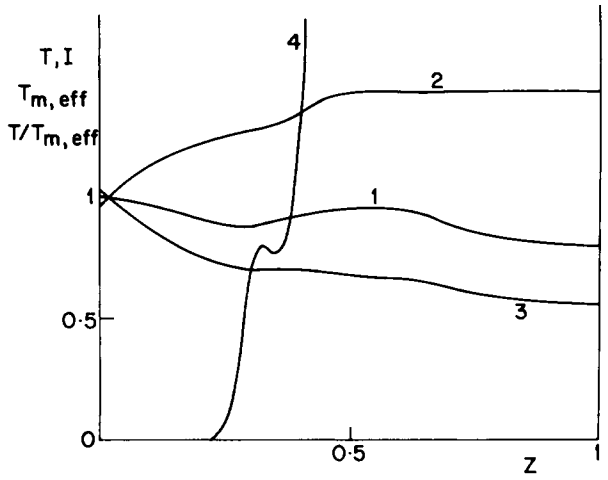

Figure 3 Temperature and rate of nucleation along a spinline; (1) T; (2) $T_{m,\text{eff}}$; (3) $T/T_{m,\text{eff}}$; (4) I; the value of nondimensional power N in (19) equals 0.1.

it is possible to calculate the scale $I^0_{\max}$ of I by using the value of K_*. The results plotted in Figures 2 and 3 correspond to the same fiber with winding velocity $V_1 = 1307.15$ m/min.

In Figure 4 the distributions of cross-section radius were plotted for various values of winding velocity. The onset of necking is clearly seen in the curve 2 and completely formed necking zones are seen in the curves 3 and 4 (the latter corresponds to the same fiber as the results plotted in Figs. 2 and 3).

The curves 3 and 4 in Figure 4 show that the configuration of cross-section radius distribution changes very slightly when high values of winding velocity V_1 have been reached. The results of calculations obtained for $V_1 = 3000$ and 6000 m/min show that the distributions of ln a are very close to the curve 4 in Figure 4 with the exception of the vicinity of point $z = 1$. There ln a sharply decreases and velocity V sharply increases to satisfy the boundary condition at a winding device. Due to the dissipative heating liquid temperature also increases in the close proximity of $z = 1$ for $V_1 = 3000$ and 6000 m/min. Obviously, the rheological model of Newtonian liquid used here is inapplicable for the description of significant stretching of fully crystallized parts of a spinline. (Only the consideration of practically nondeformable rigidlike crystalline parts of a fiber is possible as in Fig. 4). It means that to consider the highest values of V_1 (for which deformation of crystalline parts of a fiber may take place) plasticity and viscoelasticity of a crystalline fiber should be incorporated into the model.

The physical mechanism of the necking is clearly seen from Figures 2, 3, and 4. As a result of crystallization, which arises approximately at $z = 0.3$ (see curve 2 in Fig. 2) and its heat release, the liquid temperature begins to increase in spite of the convective heat removal at the fiber surface. This temperature rise is illustrated by curve 1 in Figure 3. The rise of temperature leads to the decrease of viscosity and to the appearance of a neck in the region $0.4 < z < 0.5$ (see curve 1 in Fig. 2 and curve 4 in Fig. 4). In the neck region the degree of crystallinity η_c increases sharply. This process cancels the decrease of viscosity and then leads to its growth. At the end of the necking region, the viscosity value becomes so large that the deformation of material practically ceases, the heat release due to crystallization sharply decreases, and the fiber temperature begins to decrease (see the right-hand side part of curve 1 in Fig. 3). This, in turn, leads to an increase of the overcooling, which is clearly seen from the dependence of $T/T_{m,\text{eff}}$ in Figure 3. Indeed, as the temperature T decreases and the effective melt temperature $T_{m,\text{eff}}$ is practically constant (see the right-hand side of curve 2 in Fig. 3), the ratio $T/T_{m,\text{eff}}$ decreases which manifests itself in the increase of the overcooling. As a result crystallization is rapidly completed.

Note that the dependence of $T/T_{m,\text{eff}}$ on z in Figure 3 has rather complicated character due to the competition of the heat removal, heat release in the crystallization process, and elongation. In the region

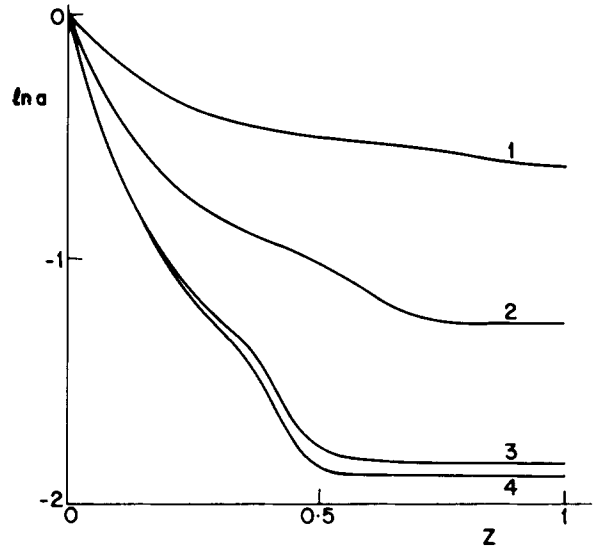

Figure 4 (1) ln a (where a is cross-section radius) for $V_1 = 100.27$ m/min; (2) 357.3 m/min; (3) 1146.95 m/min; (4) 1307.15 m/min. The value of nondimensional power N in (19) equals 0.1.

$0.25 < z < 0.45$, this dependence consecutively passes through the minimum and maximum, due to which the maximum and minimum in the rate of nucleation curve $I(z)$ appear (see curve 4 in Fig. 3). The further increase of I is related to the increase of the overcooling of a liquid. As a result, the rate of nucleation in the liquid phase sharply increases. Naturally, it takes place along with the decrease of liquid phase, since the crystallinity degree η_c permanently increases.

The dependence $I(z)$ sharply changes with the value of nondimensional power N in the nucleation law (19). In the simulation with $N = 0.253$ the dependence $I(z)$ passes consecutively twice through maximum and minimum and only afterwards does the monotonous growth of I begin. Thus, the crystallization process in the fiber as well as the necking strongly depend on the values of polymer parameters. Because of this fact, the appearance of necking in some specific range of winding velocities may be characteristic only for some specific type of polymeric liquid with rodlike molecules.

It is emphasized that the crystallization process in a spinline is practically unaffected by an increase of V_1 beyond 2000–3000 m/min.

CONCLUSIONS

A micromechanical model of nonisothermal flow-induced crystallization of rodlike molecules which allows us to describe a mutual influence of liquid flow and internal crystallization has been proposed. The results obtained with the help of this model show that the appearance of a necking zone on a fiber in high-speed spinning may be switched on by the flow-induced crystallization of rodlike polymer molecules.

Crystallization and necking processes in a spinline strongly depend on the values of polymer parameters characterizing its microstructure [first of all the power N in the nucleation law (19)]. It means that the appearance of necking in some specific range of winding velocities may be characteristic only for some specific type of rodlike molecules.

At the highest values of winding velocity there are signs of the deformation of a crystalline part of spinline. To describe this process, plasticity and viscoelasticity of a crystalline fiber should be taken into account.

The rate of crystallization in a spinline is practically unaffected by an increase in winding velocity beyond 2000–3000 m/min (for the model values of parameters used in the simulations).

This research was supported by the Center for Absorption in Science, Ministry of Immigrant Absorption (State of Israel).

REFERENCES

1. A. Ziabicki and H. Kawai (Eds.), *High-Speed Fiber Spinning*, Wiley, New York, 1985.
2. A. Ziabicki, *Fundamentals of Fibre Formation*, Wiley, New York, 1976.
3. K. F. Zieminski and J. E. Spruiell, *J. Appl. Polym. Sci.*, **35**, 2223 (1988).
4. A. Ziabicki, *J. Non-Newton. Fluid Mech.*, **30**, 157 (1988).
5. V. M. Entov and A. L. Yarin, *Dynamics of Free Jets and Films of Viscous and Rheologically Complex Liquids, Advances in Mechanics*, VINITI, *Fluid Dynamics*, Vol. 18, 112 1984 (in Russian).
6. W. Schneider, A. Koppl, and J. Berger, *Int. Polym. Process.*, **2**, 151 (1988).
7. B. Wunderlich, *Macromolecular Physics*, Academic, New York, 1976, Vol. 2.
8. L. Mandelkern, *Crystallization of Polymers*, McGraw-Hill, New York, 1964.
9. M. Doi and S. F. Edwards, *The Theory of Polymer Dynamics*, Claredon, Oxford, 1986.
10. K. E. Perepelkin, *Structure and Properties of Fibres*, Khimiya, Moscow, 1985 (in Russian).
11. A. H. Nayfeh, *Introduction to Perturbation Techniques*, Wiley, New York, 1981.

Received January 11, 1991
Accepted January 2, 1992